Electronic Spectrum and Ultraviolet Optical Properties of Crystalline MgO†

D. M. ROESSLER AND W. C. WALKER
Department of Physics, University of California, Santa Barbara, California
(Received 13 February 1967)

The electronic spectrum of single-crystal magnesium oxide, i.e., the real (ϵ_1) and imaginary (ϵ_2) parts of the dielectric response, has been obtained over the region 5–28 eV from normal-incidence reflectance spectra. Measurements were made on freshly cleaved crystals over the entire region at 295°K and from 5–11.5 eV at 77°K. Structure in ϵ_2 was observed near 7.7, 10.8, 13.3, 16.8, 17.3, and 20.5 eV. The first peak, which was found to be a doublet with components at 7.69±0.01 and 7.76±0.01 eV, was attributed to the $\Gamma_{3/2}$ and $\Gamma_{1/2}$ spin-orbit split exciton. A Lorentzian fit to the exciton components gave oscillator strengths of 0.035 and 0.017 per molecule, respectively. Subtraction of the exciton structure from the remaining interband structure gave a direct interband edge at 7.77±0.01 eV. A large plasma peak was observed in the energy-loss function near 22 eV, in agreement with recent energy-loss experiments. The remaining structure was attributed to interband transitions and will be discussed in terms of recent pseudopotential band-structure calculations.

1. INTRODUCTION

ABSOLUTE-REFLECTANCE measurements[1] on single crystals of magnesium oxide, in the range 4–15 eV, confirmed earlier work by one of us[2,3] in showing the presence of only three main peaks at room temperature. These occur at 7.60, 11.05, and 13.50 eV, respectively. Examination of the spectrum at 77°K showed none of the small features indicated by other work.[4,5] On the other hand, the exciton peak at 7.60 eV was found to sharpen considerably and exhibit doublet structure with components at 7.69 and 7.76 eV. A suggested interpretation of this feature in terms of spin-orbit interaction has been given elsewhere.[6] The remaining features below 15 eV were easily identified from an empirical pseudopotential band-structure calculation,[1] and arise from direct interband transitions. In view of the consistency between the optical properties predicted by this calculation and the experimental data it seemed worthwhile to extend the energy range of the latter. In this way, additional features of the band structure could be checked and, if necessary, the model refined for a more detailed future calculation.

In the present work, the reflectance data are extended from the previous limit of 15 to 28 eV. The Kramers-Kronig dispersion relations are used to generate the dielectric parameters which afford a more basic comparison with theory than does the reflectance. In order to define more precisely the onset for direct interband transitions at Γ, an attempt is made to subtract the contribution of the Γ exciton from the observed ϵ_2 spectrum. The next section contains a discussion of the electronic spectrum in terms of transitions predicted by the band-structure calculation. In conclusion, the computed function $\mathrm{Im}(1/\epsilon)$ is shown to be closely correlated with independent characteristic electron energy-loss work.[7,8]

2. EXPERIMENTAL PROCEDURE

The samples used were in the form of freshly cleaved single crystals, and were obtained from Semi-Elements, Inc., Pennsylvania. Further details concerning surface conditions and the accuracy of the reflectance measurements have been given elsewhere.[1,6] For the high-energy measurements, a pulsed spark discharge in argon was used. The discharge was contained in a 3-mm-diam capillary bored through boron nitride. The brass anode and cathode assemblies were water cooled, additional cooling being provided by a fan. The tip of the cathode was made of a copper-tungsten alloy to reduce sputtering during high-voltage operation. Power was supplied from a modified thyratron-tube testing unit, and a pulse rate of about 40 flashes/sec was used in practice. Under typical operating conditions, the maximum voltage was about 10 kV, with an argon flow giving about 15-μ pressure near the anode. The line emission is dense, and useful to about 450 Å in practice; the observed intensity at the exit slit is severely limited by the inefficiency at short wavelengths of the normal-incidence reflection grating in the monochromator. Full details of the power-supply unit and the reflectometer are given by Roberts.[9]

Since no window could be used to separate the reflectometer from the monochromator (the transmission limit of lithium fluoride being less than 12 eV), the possibility arises that the sample surface may become contaminated, either by discharge material carried by

† This work was supported by the National Aeronautics and Space Administration.
[1] M. L. Cohen, P. J. Lin, D. M. Roessler, and W. C. Walker, Phys. Rev. **155**, 992 (1967).
[2] D. M. Roessler, Brit. J. Appl. Phys. **16**, 1359 (1965).
[3] D. M. Roessler, Ph.D thesis, University of London, 1966 (unpublished).
[4] J. R. Nelson, Phys. Rev. **99**, 1902 (1955).
[5] G. H. Reiling and E. B. Hensley, Phys. Rev. **112**, 1106 (1958).
[6] D. M. Roessler and W. C. Walker, Phys. Rev. Letters **17**, 319 (1966).
[7] G. W. Jull, Proc. Phys. Soc. (London) **B69**, 1237 (1956).
[8] H. Raether (private communication). We are grateful to Professor Raether for permission to use these unpublished data.
[9] R. A. Roberts, Ph.D thesis, University of California, 1966 (unpublished).

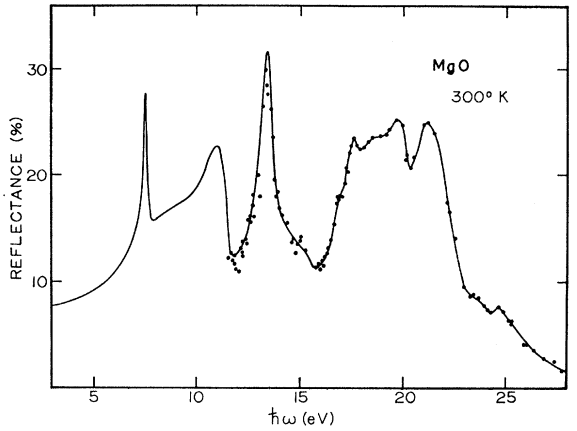

FIG. 1. Near-normal-incidence (8°) reflectance spectrum typical of a freshly cleaved crystal of MgO at 300°K.

the argon, or by back-streaming oil from the diffusion pump used to evacuate the monochromator. Previous experience[3,6] has shown that oil contamination was extremely serious when diffusion pumps were used to evacuate the reflectometer during liquid-nitrogen-temperature work. In the present case, however, no separate pumping unit was attached to the reflectometer and all measurements were made at room temperature, thereby minimizing any condensation. In practice, no decrease in reflectance was observed throughout the duration of the measurements, and it is concluded that no serious surface contamination occurred.

Although the source proved to be relatively stable, certain emission lines proved to be considerably less stable than the remainder, and intensity fluctuations could not be adequately damped in the recording system. To avoid inaccuracies from this source, as well as to reduce the usual scatter of data, both the incident and reflected spectra were recorded alternately several times for each sample. Emission lines showing intensity fluctuations of more than 5% were not used in the final calculation of the reflectance.

The measurements were made at about 8° incidence, which was considered sufficiently near normal for the purpose of analysis.

3. EXPERIMENTAL RESULTS

Figure 1 shows the reflectance of MgO from the near-ultraviolet region to 28 eV. The contribution from the back surface of the crystal (which appears in the transparent region of the spectrum, i.e., below about 7.5 eV) has been subtracted, and the low-energy tail of the 7.6-eV peak has been extrapolated to 3 eV by use of known values of the refractive index in the near-ultraviolet. Below 14 eV, the full curve denotes the data obtained from a hydrogen discharge lamp as described elsewhere.[1] Above 14 eV, the full curve represents the best fit to data obtained from the argon discharge. In the latter case, the data points are shown by the solid circles, and indicate the experimental scatter.

The new data exhibit prominent structure in the 16–23 eV region, and a marked decrease in reflectance at higher energies. The smaller features, such as the peaks at 17.6 and 24.7 eV, for example, were clearly apparent in all the measurements, even though their magnitude is little greater than the scatter. It is possible, of course, that additional structure has been obscured, if it is present in regions where the line spectrum of the source was not very dense; a gap of 0.5 eV occurs near 22 eV, for example.

For purposes of comparison with theoretical work, the most important experimental data are the values of ϵ_2, the imaginary part of the complex dielectric constant. The theoretical expression for ϵ_2, for direct interband transitions where lifetime broadening has been neglected, can be put in the form[10]

$$\epsilon_2(\omega)=\frac{e^2h^2}{m}\sum_{i,j}\frac{1}{\Omega}\int\frac{f_{ij}(\bar{k})}{E_{ij}|\nabla_k E_{ij}|}dS_k, \tag{1}$$

where

$$f_{ij}(k)=\frac{2}{3m}\frac{|\langle k,i|p|k,j\rangle|^2}{E_{ij}} \tag{2}$$

is the interband oscillator strength, S is a surface of constant interband energy, Ω is the volume of the Brillouin zone, and the interband energy $E_{ij}=E_j-E_i$.

The derivation of ϵ_2 from normal-incidence reflection data can be achieved by means of the Kramers-Kronig relations. For normal incidence, the Fresnel equations relate ϵ_2 to the reflectivity r by

$$\epsilon_2=\frac{4r(1-r^2)\sin\theta}{(1+r^2-2r\cos\theta)^2}. \tag{3}$$

The angle θ is the phase change on reflection, and is determined from the reflectance spectrum[11] by means

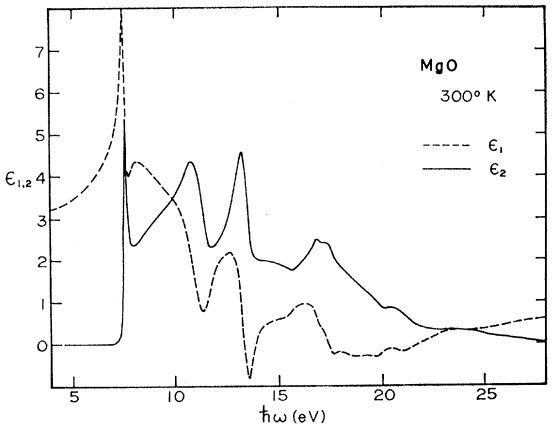

FIG. 2. The dielectric parameters ϵ_1 and ϵ_2 of MgO computed via a Kramers-Kronig analysis of the reflectance data of Fig. 1.

[10] J. C. Phillips, in *Solid State Physics*, edited by F. Seitz and D. Turnbull (Academic Press Inc., New York, 1966), Vol. 18.
[11] T. S. Robinson, Proc. Phys. Soc. (London) **B65**, 910 (1952).

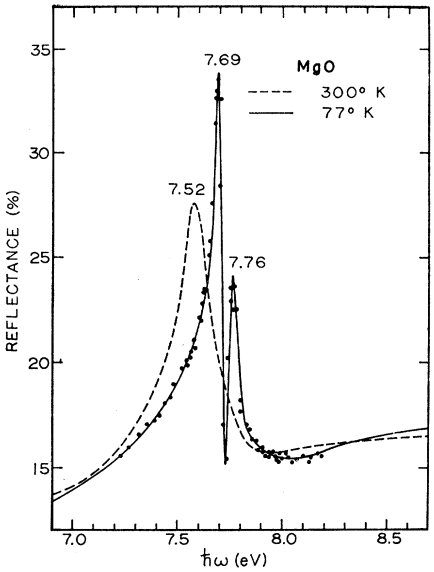

FIG. 3. Temperature dependence of the reflectance spectrum in the region of the exciton transition at Γ.

of the Kramers–Kronig integral transform:

$$\theta(\omega_0)=-\frac{1}{\pi}\int_0^\infty \ln r(\omega)\frac{d}{d\omega}\left(\ln\left|\frac{\omega+\omega_0}{\omega-\omega_0}\right|\right)d\omega. \qquad (4)$$

In principle, the whole of the reflection spectrum is therefore required to compute θ, but in practice only a limited portion is normally available. Some form of approximation is therefore necessary, and full details of the method used in the present case are given elsewhere.[12,13] The errors introduced by the computation can become important only near the end points of the experimental data. Because of extrapolation of the reflectance into the near-ultraviolet and visible region, the error is negligible here. (In theory the phase angle should be zero here; the above analysis gave a maximum error of less than 0.4°.) Above 27 eV, the errors in ϵ_2 due to the approximation are not known, but they do not affect the analysis of the spectrum given in the next section.

The computed parameters ϵ_1 and ϵ_2 are shown in Fig. 2. As expected, the shape of ϵ_2 is strongly determined by the corresponding features in the reflectance spectrum. On the other hand, the importance of ϵ_2 in determining intensities of transitions becomes clear when one examines the region above 15 eV. The strong reflectance feature between 16 and 23 eV in Fig. 1 corresponds to only a small band in ϵ_2. Beyond 20 eV, in fact, there appears to be very little interband contribution to ϵ_2.

In Fig. 3, the temperature dependence of the exciton structure below 8 eV is exhibited in detail. This feature will be discussed more fully in the next section.

[12] D. M. Roessler, Brit. J. Appl. Phys. **16**, 1119 (1965).
[13] D. M. Roessler, Brit, J. Appl. Phys. **17**, 1313 (1966).

4. ANALYSIS

The pseudopotential band calculation mentioned above[1] was programmed for only direct interband transitions and ignores the exciton transition. It is clearly useful to separate the exciton from the $\Gamma_{15}\rightarrow\Gamma_1$ edge, but the data of Fig. 2 permit only a poor estimate of the band gap—namely, 7.5±0.5 eV. An attempt was therefore made to fit the exciton structure in ϵ_2 at 77°K by a classical dispersion expression, in order to unmask the interband threshold. The computed ϵ_2 spectrum in this region at 77°K is shown in Fig. 4. The band at 7.692 ±0.003 eV is assumed to be due to the $\Gamma(j=\frac{3}{2})$ exciton, while the next highest peak is due to the exciton transition from the $j=\frac{1}{2}$ spin-orbit split valence level at Γ_{15}. The separation of the bands, about 0.07 eV, is rather large if the splitting is associated primarily with the oxygen ion, and has been discussed elsewhere.[6]

The 7.692-eV peak was fitted by a Lorentzian curve based on an isolated classical resonance; i.e.,

$$\epsilon_2=\frac{4\pi Ne^2f}{m}\frac{\Gamma\omega}{(\omega_0^2-\omega^2)^2+\Gamma^2\omega^2}, \qquad (5)$$

where the symbols have the usual connotation, f being the oscillator strength for the transition at the angular frequency of resonance ω_0, and Γ being the half-width. The result is shown by the lowest-energy dashed curve in Fig. 4. The fit is poor on the low-energy tail, but this does not seriously affect the determination of the interband threshold. From Eq. (5) it can be seen that the oscillator strength per molecule is given directly from the maximum of the $\epsilon_2\omega$ curve, since

$$f=\frac{\epsilon_2(\omega_0)\Gamma\omega_0 m}{4\pi Ne^2}. \qquad (6)$$

In the present case $\Gamma=0.038\pm0.002$ eV, and $f=0.035$ per molecule. After subtraction of this band from the

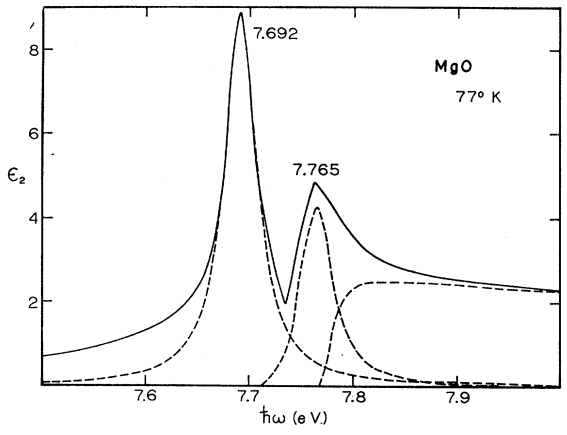

FIG. 4. The ϵ_2 spectrum at 77°K due to the Γ exciton and the threshold for interband transitions. The full curve represents the experimental data as computed from the reflectance. The dashed curves denote a possible separation into exciton and interband transitions as explained in the text.

background, a similar procedure is applied to the remaining peak at 7.765 eV. The half-width happens to be the same as for the first band, but the oscillator strength is about 0.017 per molecule. The relative intensities of the two exciton bands are therefore consistent with the spin-orbit split exciton model suggested. Separation of the second band from the background reveals the interband contribution to ϵ_2 as shown in Fig. 4. The threshold is therefore 7.77 ± 0.01 eV. Although the above procedure is somewhat crude, the resultant values for the exciton peaks and half-widths, as well as the band gap, are probably good guides to the true ones.

The binding energy for the $\Gamma(j=\frac{3}{2})$ exciton is 0.08 eV, suggesting that a Wannier model may be suitable. Thus the exciton in MgO is very much less tightly bound than is the coresponding exciton in the alkali halides, by a factor of 5 or more. The reduced mass ratio μ/m is also very small, as given by the expression

$$B=\frac{\mu e^4}{2\hbar^2\epsilon^2}=\frac{13.6}{\epsilon^2}\frac{\mu}{m}(\text{eV}), \tag{7}$$

where the binding energy B is expressed in terms of the dielectric constant ϵ and the effective mass μ. If the optical value of ϵ is taken as appropriate for the excitation, then the value of μ/m is 0.05. The nth Bohr radius is given by

$$a_n=\frac{\hbar^2\epsilon n^2}{\mu e^2}=\frac{0.529}{\mu/m}\epsilon n^2(\text{Å}). \tag{8}$$

The radius of the $n=1$ exciton is therefore 30.5 Å, or nearly fifteen times the interionic spacing (2.1Å). Knox[14] has discussed situations where the static or low-frequency value of ϵ should be used in the above formulas, rather than the optical value. In the present case, if ϵ is chosen as 9.8 rather than 2.95, the values of μ/m and the first radius are then drastically altered to 0.65 and 8 Å, respectively. An independent determination of the effective mass would enable a correct value of ϵ to be chosen. It is interesting to note that the weak binding of the Γ exciton may be a factor in the large spin-orbit splitting observed.[6]

On the assumption that the Wannier model is appropriate, a series of exciton lines from the $j=\frac{3}{2}$ valence band level should be present, where the position of the nth member is given by

$$\hbar\omega_n=7.77-0.08/n^2. \tag{9}$$

The second member should therefore lie near 7.75 eV and, if present, is obscured by the $\Gamma(j=\frac{1}{2})$ exciton at 7.765 eV. It is very improbable that the latter band may itself be the $n=2$ member of the $\Gamma(j=\frac{3}{2})$ series, since the intensity of the members is theoretically predicted to fall off as n^{-3}.[15] As indicated above, the observed intensity ratio is about $\frac{1}{2}$ instead of $\frac{1}{8}$.

The interband oscillator strength, defined by Eq. (2), is not expected to be the dominant factor in determining $\epsilon_2(\omega)$ in the case of insulators.[10] From Eq. (1) it can be seen that structure in $\epsilon_2(\omega)$ occurs at critical points where $\nabla_k E_{ij}=0$; i.e., the ith and jth bands are parallel. In the present case, therefore, it is assumed that these critical points produce the Van Hove singularities[16,17] in $\epsilon_2(\omega)$ responsible for the prominent optical structure. In the case of the $\Gamma_{15}\rightarrow\Gamma_1$ edge, the transition is expected to produce an M_0 critical point. The theoretical shape for the edge is of the form

$$\epsilon_2(\omega)=A(\hbar\omega-7.77)^{1/2}. \tag{10}$$

Examination of the edge shown in Fig. 4 gives a value for A of about 14. It is doubtful if this is significant, in view of the very crude methods used to examine the edge, but it is interesting that an expression of the form in Eq. (10) fits the experimental data rather well. The exact relationship is undoubtedly more complex, since not only has the fact been ignored that the exciton weakens the interband oscillator strength, but also the variation of the latter has been neglected in Eq. (1).

In the original band-structure calculation, the $\Gamma_{15}\rightarrow\Gamma_1$ transition was placed at 8.15 eV, whereas the above data places the M_0 edge at 7.77 eV. This should not seriously affect the basic identification of the structure previously suggested, which assigns the optical features in the 10–12 eV range to the Λ line and the L point of the Brillouin zone. The $L_3\rightarrow L_2'$ transition produces an M_0 critical point, and explains the increase in ϵ_2 beyond the contribution from the $\Gamma_{15}\rightarrow\Gamma_1$ transition. A single critical point cannot produce a peak in the joint density of states for interband transitions, however, and the peak at 10.8 eV in ϵ_2 should be associated with a strong M_1 critical point, due to the $\Lambda_3\rightarrow\Lambda_1$ transition at energies just above the $L_3\rightarrow L_2'$ threshold—which is probably in the 10.0 to 10.5 eV range. The original calculations[1] placed $L_3\rightarrow L_2'$ at 11.3 eV, and $\Lambda_3\rightarrow\Lambda_1$ at 11.4 eV, with an uncertainty of a few tenths of an electron volt. The values are therefore about 5% too high—which is the error in placing $\Gamma_{15}\rightarrow\Gamma_1$ at 8.15 eV rather than at 7.77 eV.

The $X_5'\rightarrow X_1$ transition is associated with an M_0 edge and produces the increase in ϵ_2 following the minimum at 11.8 eV. It is difficult to locate the edge precisely from the data of Fig. 2; its likely position is between 11.5 and 12 eV. This is about 5% below the calculated value (12.4 eV) for reasons given above. The peak at 13.25 eV arises from a near degeneracy of the M_1 and M_2 edges, associated with the $\Delta_5\rightarrow\Delta_1$ and $\Sigma_4\rightarrow\Sigma_1$ transitions, respectively. The calculated values of 13.2 eV for $\Delta_5\rightarrow\Delta_1$ and 13.6 eV for $\Sigma_4\rightarrow\Sigma_1$ are

[14] R. S. Knox, *Theory of Excitons* (Academic Press Inc., New York, 1963).

[15] R. J. Elliott, Phys. Rev. **108**, 1384 (1957).
[16] L. Van Hove, Phys. Rev. **89**, 1189 (1953).
[17] J. C. Phillips, Phys. Rev. **104**, 1263 (1956).

probably reliable since the position of the reflectance peak in this region was used as a basic parameter in the band-structure computation.

The only strong structure remaining lies between 15 and 18 eV. The increase in ϵ_2 beyond 15.7 eV is assigned to the M_0 edge produced by the $X_5' \rightarrow X_3$ transition. The separation of the X_1 and X_3 conduction-band levels is therefore about 4.0±0.5 eV. The separation at L, between L_2' and L_3', is nearly twice this. The $\Gamma_{15} \rightarrow \Gamma_{25}'$ transition also produces an M_0 edge in this region and should be assigned to the 16.0±0.5 eV region. At these energies, excitation can occur across the energy gaps at most of the high-symmetry points in the Brillouin zone, and the resultant structure in ϵ_2 probably arises from a number of different transitions, making a precise analysis difficult. Thus it is possible that an M_1 edge followed by an M_2 edge, both of which arise from saddle-points in the interband density of states, are responsible for the 16.8- and 17.3-eV features. The actual situation may involve more than two transitions, however, and the above must be regarded as tentative. Similarly, the structure at 20.5 eV must remain unidentified at this stage, though it probably involves transitions to the higher conduction band levels, such as L_3'.

The lack of strong structure beyond 21 eV suggests that most of the oscillator strength available for direct interband transitions has already been exhausted in the energy range below 20 eV.

5. ENERGY-LOSS SPECTRUM

It is worth examining whether the valence-band electrons contribute to a bulk plasma resonance above 20 eV. The energy losses suffered by electrons transmitted through thin films of materials can be described[18] by the function $\mathrm{Im}(1/\epsilon)$, where the dielectric response function ϵ relates to electron-electron interaction, i.e., a longitudinal disturbance. On the other hand, within the random-phase approximation, it has been shown[19] that the transverse and longitudinal dielectric responses can be described by the same parameter, ϵ, in the long-wavelength limit. The loss function $\epsilon_2/(\epsilon_1^2+\epsilon_2^2)^2$ was computed from the reflectance data of Fig. 1 and appears in Fig. 5. Since the loss curve also reflects single-particle excitations, not all the structure observed corresponds to plasma-resonance phenomena. For example, the features at 7.8, 11.6, and 13.9 eV are associated with the corresponding optical losses shown in ϵ_2 (Fig. 2). The dominant structure, namely, the band at 22.2 eV, is almost certainly due to a bulk plasma resonance in MgO, however.

A number of measurements[20,21] have been reported of the characteristic electron energy losses in thin films of MgO. For example, Watanabe[21] observed the energy spectrum of 22-keV electrons after their passage through a 200 Å-thick MgO foil. A small peak near 5.5 eV was not considered to be an intrinsic property of MgO, but a second peak at 11.4 eV was taken as a measure of the first forbidden energy gap. The latter has been established as 7.77 eV in the present work, while we believe the 11.4 eV peak [which occurs in the $\mathrm{Im}(1/\epsilon)$ function in Fig. 5] to be associated with the single-particle excitation of the interband transitions $L_3 \rightarrow L_2'$, $\Lambda_3 \rightarrow \Lambda_1$. A peak found at 25 eV was attributed to a further interband transition (probably equivalent to $\Gamma_{15} \rightarrow \Gamma_{25}'$) involving the highest-valence band level and one of the higher-lying conduction bands. It is more probable that Watanabe was really seeing the bulk plasma loss, which appears at 22.2 eV in Fig. 5. The poorer resolution of his electron energy-loss work would prevent observation of the small peak appearing at 24.7 eV in Fig. 5, and which should be assigned to interband transitions.

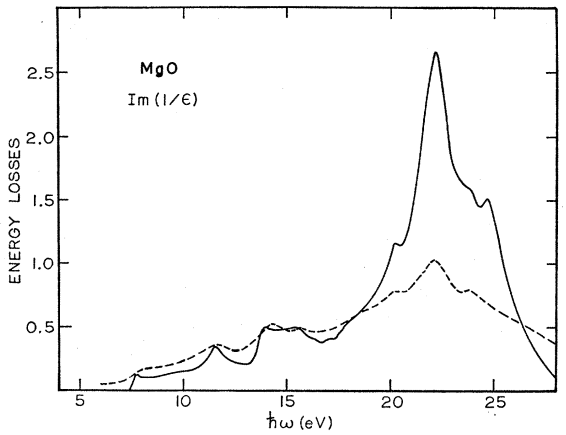

FIG. 5. The energy-loss function of MgO, $\mathrm{Im}(1/\epsilon)$, as computed from reflectance data, is shown by the full curve. The broken curve shows the electron energy losses measured by von Festenberg.

Jull's work[7] with 10-keV electrons exhibits a strong loss at 22.5 eV, in good agreement with the present data. Some higher-resolution work on electron energy losses is being done by Raether's group at the University of Hamburg.[8] Absolute values have recently been measured by von Festenberg on MgO films, produced by oxidizing metallic magnesium, and are shown by the broken curve in Fig. 5. The agreement between the loss spectra is excellent, both in absolute magnitude and in spectral structure, emphasizing the validity of the random-phase approximation for ϵ. The only discrepancy occurs near the bulk plasma loss, but even here the structure is preserved in both curves. The reason for the difference in absolute magnitudes at the plasma peak is not clear, and may arise from the method of preparation of the MgO samples used in the electron energy-loss work.

[18] H. Fröhlich and H. Pelzer, Proc. Phys. Soc. (London) **A68**, 525 (1955).
[19] S. L. Adler, Phys. Rev. **126**, 413 (1962).
[20] E. Rudberg, Proc. Roy. Soc. (London) **A127**, 111 (1930).
[21] H. Watanabe, Phys. Rev. **95**, 1684 (1954).

If the loss at 22.2 eV is due to collective excitation of the valence-band electrons it is simple to estimate the theoretical plasma frequency ω_p from the expression

$$\omega_p^2 = 4\pi Ne^2/m. \quad (11)$$

If only the 6 electrons in the O—$2p$ valence band are included, then $\hbar\omega_p$ is about 21 eV. In view of the simplicity of this model, the agreement with experiment is good. Since interband transitions are also occurring in this region, though weakly, the actual plasma resonance may be shifted from the free-electron plasma energy in any case, as has been pointed out by Wilson.[22]

[22] C. B. Wilson, Proc. Phys. Soc. (London) **76**, 481 (1960).

In considering plasma oscillations in metals, both Wolff[23] and Kanazawa[24] derive an expression governing the half-width for the resonance in the form

$$\hbar\Gamma/\hbar\omega_p = nk. \quad (12)$$

It is difficult to determine the half-width of the resonance in Fig. 5, because of the proximity of losses due to interband transitions (at 20.3, 23.9 and 24.7 eV, for example). It appears to be about 3 eV, however, and therefore the ratio of half-width to plasma frequency (22.2 eV) is 0.14. This is of the right magnitude since, in practice, $\epsilon_2/2$ is about 0.18 at 22.2 eV.

[23] P. A. Wolff, Phys. Rev. **92**, 18 (1953).
[24] H. Kanazawa, Progr. Theoret. Phys. (Kyoto) **13**, 227 (1955)

PHYSICAL REVIEW VOLUME 159, NUMBER 3 15 JULY 1967

Calculation of the Spin-Orbit Parameters for the Valence Bands of the fcc Alkali Chlorides, Alkali Bromides, and Alkali Iodides*

A. Barry Kunz
Department of Physics, Lehigh University, Bethlehem, Pennsylvania
(Received 24 February 1967)

The spin-orbit parameters for the fcc alkali chlorides, alkali bromides, and alkali iodides have been calculated. Tight-binding wave functions and potentials of a type used in earlier calculations by the author were used. Various overlap corrections were computed; of these the only significant one was found to be the correction to the normalization of the wave functions due to overlap. The theoretical spin-orbit splittings for the point Γ in the first Brillouin zone, obtained by the assumption of LS coupling, were found to compare favorably with existing optical data.

I. INTRODUCTION

In the past few years, calculations on the structure of the valence bands of the alkali halides have become very refined. In many cases such corrections as spin-orbit effects have been included.[1–5] There have also been recent attempts by Phillips[6] to relate the results of band-structure calculations to the measured spectra of these substances. The results of these interpretations have proved somewhat controversial,[3,7] and this points out the need for more study of the band structure of the alkali halides. Even for substances such as the alkali chlorides, where the spin-orbit splittings are small, one should include these effects in a band-structure calculation, if one is to attempt to relate the results of the calculation to the existing spectral data. The necessity of including spin-orbit corrections in the alkali iodides is obvious, because their magnitude is of the order of 1 eV. In fact, the size of the splitting in the NaI valence band, which is 1.25 eV at the Γ point, has only recently been satisfactorily explained.[5]

There have been other recent calculations on other chlorides, some of which do not include spin-orbit results but which are complete in other respects.[8–10] It is possible to modify these results to include spin-orbit effects by the use of perturbation theory. To do this, one would obtain band structures in the tight-binding formulation of Slater and Koster[11] by performing a curve fitting for the available bands. In this paper, tight-binding theory is assumed, and spin-orbit parameters have been calculated for the various fcc alkali chlorides, alkali iodides, and alkali bromides.

* Work supported in part by the U. S. Atomic Energy Commission under Contract No. AT-(30-1)-3408.
[1] Y. Onodera and M. Okazaki, J. Phys. Soc. Japan **21**, 1273 (1966).
[2] Y. Onodera, M. Okazaki, and T. Inui, J. Phys. Soc. Japan **21**, 816 (1966).
[3] Y. Onodera, M. Okazaki, and T. Inui, Tech. Rept. Inst. Solid State Phys., Univ. Tokyo **A209** (1966).
[4] A. Barry Kunz and W. J. Van Sciver, Phys. Rev. **142**, 462 (1966).
[5] A. Barry Kunz, Phys. Rev. **151**, 620 (1966).
[6] J. C. Phillips, Phys. Rev. **136**, A1705 (1964).
[7] R. S. Knox (private communication).
[8] L. P. Howland, Phys. Rev. **109**, 1927 (1956).
[9] F. Bassani, R. S. Knox, and W. Beall Fowler, Phys. Rev. **132**, A1217 (1965).
[10] P. DeCicco, Solid State and Molecular Theory Group, M.I.T., Quarterly Progress Report No. 56, 1965, p. 49 (unpublished).
[11] J. C. Slater and G. F. Koster, Phys. Rev. **94**, 1498 (1954).